

Analytical Study Based Optimal Placement of Energy Storage Devices in Power Systems to Support Voltage and Angle Stability

Mehdy Khayamy^{‡1}, Adel Nasiri¹, and Farhad Balali¹

¹Center for Sustainable Electrical Energy Systems, University of Wisconsin-Milwaukee of Milwaukee, Wisconsin, USA

¹mkhayamy@uwm.edu, nasiri@uwm.edu, mbalali@uwm.edu

[‡]Corresponding Author: mkhayamy@uwm.edu, Phone number: (931)529-1889

Received: 27.09.2019 Accepted: 22.10.2019

Abstract-Larger penetration of Distributed Generations (DG) in the power system brings new flexibility and opportunity as well as new challenges due to the generally intermittent nature of DG. When these DG are installed in the medium voltage distribution systems as components of the smart grid, further support is required to ensure a smooth and controllable operation. To complement the uncontrollable output power of these resources, energy storage devices need to be incorporated to absorb excessive power and provide power shortage in time of need. They also can provide reactive power to dynamically help the voltage profile. Energy Storage Systems (ESS) can be expensive and limited number of them can practically be installed in distribution systems. In addition to frequency regulation and energy time shifting, ESS can support voltage and angle stability in the power network. This paper applies a Jacobian matrix-based sensitivity analysis to determine the most appropriate node in a grid to collectively improve the voltage magnitude and angle of all the nodes by active/reactive power injection. IEEE 14, 24, and 123-bus distribution system are selected to demonstrate the performance of the proposed method. As opposed to most previous studies, this method does not require an iteration loop with a convergence problem nor a network-related complicated objective function.

Keywords Distributed generations; energy storage; Jacobian matrix; optimal placement; sensitivity analysis; smart grid.

1 Introduction

Classic distribution systems (DS) have grid connected feeders and several radial networks. Remote loads from the feeders experience larger voltage drops and angle differences. Local active and reactive power support can improve voltage magnitude and angle profile. To compensate for the voltage drop and to reduce line loss, shunt capacitors have traditionally been installed. The capacitors are constant and can be switched in steps and, therefore, the reactive power cannot be continuously controlled. However, an optimal placement can be conducted to maximize the impact. Both the fuzzy-based approach and genetic algorithm [1] have been used to determine the optimal placement of these fixed capacitor banks in radial distribution networks for a relatively small size test network of IEEE 18-Bus system [2, 3]. The battery placement optimization has been done via network framework as well [4]. Sometimes the battery placement is only one goal of a multi-objective optimization [5].

Optimal placement of generators is usually investigated for the transmission systems and it is one of the key performance index of the grid [6]. In the literature, the optimization studies started on a small 5-bus systems to 18, 24, 30, and 34

bus-systems [7, 8, 9, 10, 11]. The method of optimization is usually the genetic algorithm [9, 10, 12] or optimizing objective functions on an iteration loop [7, 10, 11]. For larger network, there are slower iteration loops and additional concern on convergence. In the case of wind farm placement, statistical wind data need to be incorporated into the goal function as well [9, 10]. Furthermore, exchangeable batteries for dynamic capacity changing has been studied [13].

There is an increasing penetration of DG in the distribution system due to their inherent merits offering several advantages over central large power plants. Nevertheless, DG adversely impact the distribution system in several ways. They may lead to power and voltage fluctuations and degradation of power quality [14]. Another challenge in utilizing DG is the generally intermittent nature of their generation. It pressures the utility connection to keep the balance of the load and generation and energy management algorithm [15]. Uncertainty in the DG network is one of the most challenging areas since the supply and demand are both uncertain and the nature of the available information such as electricity prices, load demand, and regulation signals are all stochastic [16].

As the share of DG increases in the distribution systems, re-

source forecasting becomes more important to control or mitigate the fluctuations in generation [17]. Installing ESS in the system leads to increasing both the reliability and efficiency of the systems. The demand and generation predictions are usually a day ahead or real time to achieve a specific level of the system reliability. These predictions determine the different characteristics and schedules of the generators and ESS to maintain the balance between demand and supply [18, 19]. The fast-response ESS are responsible for the hourly power variation, whereas the slow-response ESS coordinate with the energy shortage or surplus [20]. Furthermore, ESS have various functions including peak shaving, voltage regulation, frequency regulation, etc. which all can be achieved considering the ESS as components of the DG system [21]. Several studies have been conducted to investigate the effect of ESS on the overall cost of electricity [22, 20, 23].

An ESS coupled with an inverter can significantly affect the fluctuations of the voltage magnitude and angle and provide the active and reactive power for the DG system [14, 24]. ESS are connected to the distribution network through the inverters and hence the system is capable of absorbing/providing both active and reactive powers. ESS can address both power oscillation and voltage drop problems. Since ESS are capable of immediately changing the direction of active/reactive power, they can compensate for momentary unpredictable nature of DG and balance the source/load generation, rendering relatively constant demand from the utility [25].

Another reason of installing ESS is to defer network upgrade. They can defer the upgrades to twice as long as the network without ESS [26]. In this case, the optimal placement method must consider increased loads at various nodes to observe the impacts of future load growth.

There are different approaches for finding the optimal place of an ESS and usually the main objective of the problem is to find the optimal place for an ESS to minimize the installation and operating cost while maintaining the power and voltage at desired level. Obviously, the least number of the ESS which can meet the technical requirement is more favorable.

This paper suggests an analytical method to determine the optimal place of an ESS. Since the method does not require an iteration loop for the goal function, it can be applied to large-scale distribution networks as well. The size of the test system in most of the papers is usually 18-24 nodes and one paper implemented their method for a 69-node system [27]. Recently, some analytical methods are developed that rely on the formulation of the problem rather than iteration loop but since the formulation is complicated the system is tested only on a 7-node system [28]. The main advantages of the problem formulation over the other methods are independency of the iteration loop and consequently, no issues with the convergence of the problem.

This paper proposes a novel algorithm in the medium voltage network based on the Jacobian matrix to find the optimal place of the ESS. The goal of the algorithm is to detect the weakest nodes of the network which might be excellent candidates for placing the energy storage devices. The weakest node of the network is a node which has the maximum sensitivity of the

voltage magnitude and angle given under the same active and reactive power to the system.

2 Jacobian Matrix as the Sensitivity Index

There are several algorithms to calculate the power flow and due to the nonlinear nature of the system, they are based on iteration loop. Newton-Ralphson is the most optimal method because it uses the Jacobian sensitivity matrix, J , and requires the least iteration to converge and there are still enhancements to be done on the power flow method to address singularity and convergence issues in smart grids [29]. Although building J from a network configuration (Y-bus) and condition (power and voltage values of the buses) is a fundamental part of the Newton-Ralphson method to perform the power flow, J can be used in other studies as well.

If m is the number of PV nodes, n is the number of PQ nodes, and t is the total number of nodes then considering one slack node, $t = m + n + 1$. Equation (1) shows J as it describes how much variation in the bus voltage angle and magnitude translates the active and reactive power. J includes four submatrices which are shown in (1). Due to the strong relation between the active power, P , and the voltage angles, δ , on one hand, and the reactive power, Q , and the voltage magnitude, $|V|$, on the other hand, $J_{P\delta}$ and J_{QV} are important submatrices compared to J_{PV} and $J_{Q\delta}$ which relate P to V and Q to δ respectively.

J has proven its power by optimal solving of power flow problem but to use it for the optimal placement of the ESS, J needs to be restructured. While J is describing the effect of δ and $|V|$ on the P and Q , an ESS can provide/absorb the power and therefore an ideal tool should describe the effect of power on δ and $|V|$ to find the weakest node of the network. This tool is the inverse of the Jacobian matrix as it is shown in equation (2). For any non-singular network, J^{-1} exists and similar to J in can be divided into four submatrices. The detailed relation between δ , $|V|$, P , and Q is shown in (2).

Boundaries to divide J^{-1} into four submatrices are as follows:

$$J'_{\delta P (m+n) \times (m+n)} = J'^{-1}([1 : t-1], [1 : t-1]) \quad (3a)$$

$$J'_{\delta Q (m+n) \times n} = J'^{-1}([1 : t-1], [t : t-1+n]) \quad (3b)$$

$$J'_{VP n \times (m+n)} = J'^{-1}([t : t-1+n], [1 : t-1]) \quad (3c)$$

$$J'_{VQ n \times n} = J'^{-1}([t : t-1+n], [t : t-1+n]) \quad (3d)$$

Although most of the nodes in a distribution system are PQ , there are some PV nodes which have direct utility connection. Usually, the function of an ESS in the distribution system is not to provide power for all of the loads and utility connection is always required. The battery provides some active or reactive power to the weak nodes of the network in times and hence they are usually far from the utility connection. If a battery connected

$$\begin{pmatrix} \Delta P_2 \\ \Delta P_3 \\ \vdots \\ \Delta P_t \\ - \\ \Delta Q_2 \\ \Delta Q_3 \\ \vdots \\ \Delta Q_t \end{pmatrix} = \begin{pmatrix} \frac{\partial P_2}{\partial \delta_2} & \frac{\partial P_2}{\partial \delta_3} & \dots & \frac{\partial P_2}{\partial \delta_t} & | & \frac{\partial P_2}{\partial |V_2|} & \frac{\partial P_2}{\partial |V_3|} & \dots & \frac{\partial P_2}{\partial |V_t|} \\ \frac{\partial P_3}{\partial \delta_2} & \frac{\partial P_3}{\partial \delta_3} & \dots & \frac{\partial P_3}{\partial \delta_t} & | & \frac{\partial P_3}{\partial |V_2|} & \frac{\partial P_3}{\partial |V_3|} & \dots & \frac{\partial P_3}{\partial |V_t|} \\ \vdots & \vdots & \ddots & \vdots & | & \vdots & \vdots & \ddots & \vdots \\ \frac{\partial P_t}{\partial \delta_2} & \frac{\partial P_t}{\partial \delta_3} & \dots & \frac{\partial P_t}{\partial \delta_t} & | & \frac{\partial P_t}{\partial |V_2|} & \frac{\partial P_t}{\partial |V_3|} & \dots & \frac{\partial P_t}{\partial |V_t|} \\ - & - & - & - & | & - & - & - & - \\ \frac{\partial Q_2}{\partial \delta_2} & \frac{\partial Q_2}{\partial \delta_3} & \dots & \frac{\partial Q_2}{\partial \delta_t} & | & \frac{\partial Q_2}{\partial |V_2|} & \frac{\partial Q_2}{\partial |V_3|} & \dots & \frac{\partial Q_2}{\partial |V_t|} \\ \frac{\partial Q_3}{\partial \delta_2} & \frac{\partial Q_3}{\partial \delta_3} & \dots & \frac{\partial Q_3}{\partial \delta_t} & | & \frac{\partial Q_3}{\partial |V_2|} & \frac{\partial Q_3}{\partial |V_3|} & \dots & \frac{\partial Q_3}{\partial |V_t|} \\ \vdots & \vdots & \ddots & \vdots & | & \vdots & \vdots & \ddots & \vdots \\ \frac{\partial Q_t}{\partial \delta_2} & \frac{\partial Q_t}{\partial \delta_3} & \dots & \frac{\partial Q_t}{\partial \delta_t} & | & \frac{\partial Q_t}{\partial |V_2|} & \frac{\partial Q_t}{\partial |V_3|} & \dots & \frac{\partial Q_t}{\partial |V_t|} \end{pmatrix} \begin{pmatrix} \Delta \delta_2 \\ \Delta \delta_3 \\ \vdots \\ \Delta \delta_t \\ - \\ \Delta |V_2| \\ \Delta |V_3| \\ \vdots \\ \Delta |V_t| \end{pmatrix}, \quad \begin{pmatrix} \Delta P \\ \Delta Q \end{pmatrix} = \begin{pmatrix} \frac{\partial P}{\partial \delta} & \frac{\partial P}{\partial |V|} \\ \frac{\partial Q}{\partial \delta} & \frac{\partial Q}{\partial |V|} \end{pmatrix} \begin{pmatrix} \Delta \delta \\ \delta |V| \end{pmatrix} \quad (1)$$

$$J = \begin{pmatrix} J_{P\delta} (m+n) \times (m+n) & J_{PV} (m+n) \times n \\ J_{Q\delta} n \times (m+n) & J_{QV} n \times n \end{pmatrix}$$

$$J_{(m+2n) \times (m+2n)}$$

$$\begin{pmatrix} \Delta \delta_2 \\ \Delta \delta_3 \\ \vdots \\ \Delta \delta_t \\ - \\ \Delta |V_2| \\ \Delta |V_3| \\ \vdots \\ \Delta |V_t| \end{pmatrix} = \begin{pmatrix} \frac{\partial \delta_2}{\partial P_2} & \frac{\partial \delta_2}{\partial P_3} & \dots & \frac{\partial \delta_2}{\partial P_t} & | & \frac{\partial \delta_2}{\partial Q_2} & \frac{\partial \delta_2}{\partial Q_3} & \dots & \frac{\partial \delta_2}{\partial Q_t} \\ \frac{\partial \delta_3}{\partial P_2} & \frac{\partial \delta_3}{\partial P_3} & \dots & \frac{\partial \delta_3}{\partial P_t} & | & \frac{\partial \delta_3}{\partial Q_2} & \frac{\partial \delta_3}{\partial Q_3} & \dots & \frac{\partial \delta_3}{\partial Q_t} \\ \vdots & \vdots & \ddots & \vdots & | & \vdots & \vdots & \ddots & \vdots \\ \frac{\partial \delta_t}{\partial P_2} & \frac{\partial \delta_t}{\partial P_3} & \dots & \frac{\partial \delta_t}{\partial P_t} & | & \frac{\partial \delta_t}{\partial Q_2} & \frac{\partial \delta_t}{\partial Q_3} & \dots & \frac{\partial \delta_t}{\partial Q_t} \\ - & - & - & - & | & - & - & - & - \\ \frac{\partial |V_2|}{\partial P_2} & \frac{\partial |V_2|}{\partial P_3} & \dots & \frac{\partial |V_2|}{\partial P_t} & | & \frac{\partial |V_2|}{\partial Q_2} & \frac{\partial |V_2|}{\partial Q_3} & \dots & \frac{\partial |V_2|}{\partial Q_t} \\ \frac{\partial |V_3|}{\partial P_2} & \frac{\partial |V_3|}{\partial P_3} & \dots & \frac{\partial |V_3|}{\partial P_t} & | & \frac{\partial |V_3|}{\partial Q_2} & \frac{\partial |V_3|}{\partial Q_3} & \dots & \frac{\partial |V_3|}{\partial Q_t} \\ \vdots & \vdots & \ddots & \vdots & | & \vdots & \vdots & \ddots & \vdots \\ \frac{\partial |V_t|}{\partial P_2} & \frac{\partial |V_t|}{\partial P_3} & \dots & \frac{\partial |V_t|}{\partial P_t} & | & \frac{\partial |V_t|}{\partial Q_2} & \frac{\partial |V_t|}{\partial Q_3} & \dots & \frac{\partial |V_t|}{\partial Q_t} \end{pmatrix} \begin{pmatrix} \Delta P_2 \\ \Delta P_3 \\ \vdots \\ \Delta P_t \\ - \\ \Delta Q_2 \\ \Delta Q_3 \\ \vdots \\ \Delta Q_t \end{pmatrix}, \quad \begin{pmatrix} \Delta \delta \\ \Delta |V| \end{pmatrix} = \begin{pmatrix} \frac{\partial \delta}{\partial P} & \frac{\partial \delta}{\partial Q} \\ \frac{\partial |V|}{\partial P} & \frac{\partial |V|}{\partial Q} \end{pmatrix} \begin{pmatrix} \Delta P \\ \Delta Q \end{pmatrix} \quad (2)$$

$$J'^{-1} = \begin{pmatrix} J'_{\delta P} (m+n) \times (m+n) & J'_{\delta Q} (m+n) \times n \\ J'_{VP} n \times (m+n) & J'_{VQ} n \times n \end{pmatrix}$$

$$J'^{-1}_{(m+2n) \times (m+2n)}$$

to the same bus of utility connection, all of the roles of the battery can be done by utility itself and so PV nodes do not need an ESS and the rows and columns related to these nodes have to be removed from J'^{-1} submatrices. As the dimension of submatrices are mentioned in equation (2), $J'_{\delta P}$ has PV rows and columns, $J'_{\delta Q}$ has PV rows, J'_{VP} has PV columns and J'_{VQ} does not have any PV row or column. Four n by n matrix have to be extracted from $J'_{\delta P}$, $J'_{\delta Q}$, J'_{VP} , and J'_{VQ} which excludes PV rows and columns. These square n by n matrices are called $J_{\delta P}$, $J_{\delta Q}$, J_{VP} , and J_{VQ} . The elimination process is shown in Fig. ?? for IEEE-14 bus system. The gray cells have to be eliminated. The reduced Jacobian matrix inverse is shown in equation (5).

$$\begin{pmatrix} \Delta \delta \\ \Delta |V| \end{pmatrix} = \begin{pmatrix} J_{\delta P} & J_{\delta Q} \\ J_{VP} & J_{VQ} \end{pmatrix} \begin{pmatrix} \Delta P \\ \Delta Q \end{pmatrix} \quad (4)$$

$$J_{2n \times 2n}^{-1} = \begin{pmatrix} J_{\delta P} n \times n & J_{\delta Q} n \times n \\ J_{VP} n \times n & J_{VQ} n \times n \end{pmatrix} \quad (5)$$

Although $J_{\delta P}$ and J_{VQ} are dominant matrices, the effect of $J_{\delta Q}$ and J_{VP} have to be considered as well. From the active power point of view, the best node to install an ESS is the one

who has the maximum δ recovery after the injection of a certain P . On the other hand, from the reactive power point of view, the best node is the one who has the maximum voltage drop, $|V|$, recovery after the injection of a certain Q . These concepts can be combined together in the next section.

3 Criteria for the Most Vulnerable Node Detection

For a certain amount of power variation in the system, the angle and magnitude of a weak node deviates more than strong node and therefore they are vulnerable and more prone to instability. Beside the four primary raw matrix indexes of $J_{\delta P}$, $J_{\delta Q}$, J_{VP} , and J_{VQ} , other indexes can be defined to translate P and Q to δ and V in more meaningful ways. Because of the strong relation between active power and the voltage angle on the one side and the strong relation between reactive power and the voltage magnitude on the other side, usually the active power is getting injected to overcome the angle deviation and the reactive power to compensate the voltage drop. One of the specifications of an ideal node to install ESS from the control point of view is to have decoupled relation between P and δ or Q and V . These nodes

are attractive because the active power can highly influence the angle but does not affect the magnitude by much and the reactive power mainly impact the magnitude rather than the angle.

There are several matrix indexes which can be defined to show the weakest decoupled node. Equation (6) shows the first compound matrix index set. J_P shows how much active power can influence the angle but not the magnitude of nodes. Since numerical values of $J_{\delta P}$ are very higher than J_{VP} , for any practical system this J_P is positive. Similarly, J_Q shows how much reactive power can influence the magnitude but not the angle of nodes.

$$J_P = J_{\delta P} - J_{VP} \quad (6a)$$

$$J_Q = J_{VQ} - J_{\delta Q} \quad (6b)$$

The second compound matrix index set of (7) is the dual of the first set (6). Index matrix, J_δ , can be constructed by subtracting $J_{\delta Q}$ from $J_{\delta P}$. It is an indication for nodes with high sensitivity of the angle to active power but not reactive power. Similarly, subtracting J_{VP} from J_{VQ} leads to an index which reveals a node with high sensitivity of voltage to the reactive power but less sensitivity to the active power (J_V).

$$J_\delta = J_{\delta P} - J_{\delta Q} \quad (7a)$$

$$J_V = J_{VQ} - J_{VP} \quad (7b)$$

The total compound index is the summation of either the first set or the second set. The scaling coefficient, $k_{\delta V}$, is a design factor

It is the dominant submatrices minus the minor submatrices.

$$J_T = J_P + J_Q = J_\delta + J_V = J_{\delta P} + J_{VQ} - J_{\delta Q} - J_{VP} \quad (8)$$

Equations (6) and (7) are one way to decouple the effect of active and reactive power over the angle and magnitude. Considering the operation of the closed loop control system there is a second way to do that. To find the sensitivity effect of injected active power, on the bus voltage angle, compact form of equation (4) is extended here:

$$\Delta\delta = J_{\delta P}\Delta P + J_{\delta Q}\Delta Q \quad (9)$$

$$\Delta|V| = J_{VQ}\Delta Q + J_{VP}\Delta P \quad (10)$$

Equations (9) and (10) are in the matrix form. An ESS is connected to the network through a three-phase inverter and hence can regulate both of the $|V|$ and δ . Although $\Delta\delta$ has a strong relation to ΔP in (9), the effect of ΔQ needs to be considered as well. ΔQ can be obtained from (10):

$$\Delta Q = J_{VQ}^{-1}\Delta|V| - J_{VP}^{-1}\Delta P \quad (11)$$

and substituted back into (9) as it is shown in equation (12).

$$\Delta\delta = J_{\delta P}\Delta P + J_{\delta Q}(J_{VQ}^{-1}\Delta|V| - J_{VP}^{-1}\Delta P) \quad (12a)$$

$$\Delta\delta = (J_{\delta P} - J_{\delta Q}J_{VQ}^{-1}J_{VP})\Delta P + J_{\delta Q}J_{VQ}^{-1}\Delta|V| \quad (12b)$$

$$\Delta\delta = (J_{\delta P} - J_{\delta Q}J_{VQ}^{-1}J_{VP})\Delta P \quad (12c)$$

$$J_{\delta Pe} = J_{\delta P} - J_{\delta Q}J_{VQ}^{-1}J_{VP} \quad (12d)$$

Assuming the voltage magnitude is being kept constant by the ESS's voltage regulator loop, $\Delta|V|$ can be neglected and the sensitivity of the voltage angle to the injected active power can be described by $J_{\delta P} - J_{\delta Q}J_{VQ}^{-1}J_{VP}$. $J_{\delta P}$ is the dominant term and $J_{\delta Q}J_{VQ}^{-1}J_{VP}$ is subtracted to eliminate the effect of reactive power and create $J_{\delta Pe}$ which is the eliminated and decoupled form of $J_{\delta P}$.

Similar to the active power and the voltage angle, sensitivity of the reactive power and the voltage magnitude can be calculated as well. ΔP can be obtained from (9):

$$\Delta P = J_{\delta P}^{-1}\Delta\delta - J_{\delta P}^{-1}J_{\delta Q}\Delta Q \quad (13)$$

and substituted back into (10) as it is shown in equation (12).

$$\Delta|V| = J_{VQ}\Delta Q + J_{VP}(J_{\delta P}^{-1}\Delta\delta - J_{\delta P}^{-1}J_{\delta Q}\Delta Q) \quad (14a)$$

$$\Delta|V| = (J_{VQ} - J_{VP}J_{\delta P}^{-1}J_{\delta Q})\Delta Q + J_{VP}J_{\delta P}^{-1}\Delta\delta \quad (14b)$$

$$\Delta|V| = (J_{VQ} - J_{VP}J_{\delta P}^{-1}J_{\delta Q})\Delta Q \quad (14c)$$

$$J_{VQe} = J_{VQ} - J_{VP}J_{\delta P}^{-1}J_{\delta Q} \quad (14d)$$

Assuming the voltage angle and magnitude control loops of the inverter are independent and they react through the channels of active and reactive powers, variation of the angle can be ignored and the sensitivity of the voltage magnitude to the injected reactive power can be described by $J_{VQ} - J_{VP}J_{\delta P}^{-1}J_{\delta Q}$.

Up to this point, two criteria are defined.

- The most vulnerable bus in the sense of the active power or the best placement of P injection, equation (12).
- The most vulnerable bus in the sense of the reactive power or the best placement of Q injection, equation (14).

Since an ESS can inject both of the active and reactive powers, it has to be installed on a bus which is most vulnerable to both P and Q and therefore criteria (12) and (14) can be combined into the general node detection criteria of equation (15).

$$J_{Te} = J_{\delta P} + J_{VQ} - J_{\delta Q}J_{VQ}^{-1}J_{VP} - J_{VP}J_{\delta P}^{-1}J_{\delta Q} \quad (15)$$

Each element of $J_{\delta P}$, $\frac{\partial\delta_i}{\partial P_j}$, describes the variation in the angle of the node i after changing active power in the node j . Absolute summation of all the elements of the column i together indicates the overall effect of an injected P_i over all the voltage angles of the network. The higher variation in the voltage angles means a better place to inject an active power. This index is shown in equation (16) for any node i . Similarly, other indexes are defined in equations (17), (18), and (19) based on other submatrices of the reduced Jacobian matrix inverse. Compound Indices

are found with the similar approach of the basic indices from their corresponding index matrix.

$$I_{\delta P_i} = \sum_{k=1}^n |J_{\delta P}(k, i)| \quad (16) \quad I_{\delta Q_i} = \sum_{k=1}^n |J_{\delta Q}(k, i)| \quad (17)$$

$$I_{VP_i} = \sum_{k=1}^n |J_{VP}(k, i)| \quad (18) \quad I_{VQ_i} = \sum_{k=1}^n |J_{VQ}(k, i)| \quad (19)$$

Beside the mathematical approaches of (12) and (14), index matrices of $J_{\delta P_e}$, J_{VQ_e} , and consequently J_{T_e} can be derived in an intuitive way as well. $J_{\delta P_e}$ has a dominant part of $J_{\delta P}$ which relates $(\delta \leftarrow P)$ minus $J_{\delta Q} J_{VQ}^{-1} J_{VP} = J_{\delta Q} J_{QV} J_{VP}$ which translates P to δ through the indirect channel of V and Q as $(\delta \leftarrow Q)(Q \leftarrow V)(V \leftarrow P)$. Similarly, J_{VQ_e} eliminates indirect channel of δ and P from $J_{VQ}(V \leftarrow Q)$ by $J_{VP} J_{\delta P}^{-1} J_{\delta Q} = J_{VP} J_{P\delta} J_{\delta Q}$ which is $(V \leftarrow P)(P \leftarrow \delta)(\delta \leftarrow Q)$. Fig. ?? depicts the mentioned concept of these indices.

4 IEEE 14-Bus System as the First Test Network

The first network that the indices are applied to is IEEE 14-bus system mainly due to its simplicity and transparent result presentation. The network is shown in Fig. ?? with some indices on the nodes and the utility is connected to node 1. Fig. ?? shows four basic indices. As expected, major indices of $I_{\delta P}$ and I_{VQ} have higher values compared to minor indices of $I_{\delta Q}$ and I_{VP} . These indices are scaled to be between 0 to 100%. Fig. ?? shows the compound indices. Eliminated and decoupled indices are shown in Fig. ?. I_P , I_δ , and $I_{\delta P_e}$ on one hand and I_Q , I_V , and I_{VQ_e} on the other hand, have almost the same general trends.

According to $I_{\delta P_e}$ weak nodes are 12, 13, and 14 which are ideal if the main objective of the ESS is to manipulate the active power. Based on I_{VQ_e} weak nodes are 9, 10, and 14 which are perfect if the inverter is very over-sized compared to the DC energy storage device and it can manipulate the reactive power. There are similarities between the total compound index of I_T and the total eliminated index of I_{T_e} . The suggested nodes for an ESS which needs to manipulate both of the active and reactive power is either node 10 or 14.

Although cumulative indices of I_T and I_{T_e} have similar trends, one of them should be selected as the benchmark. An ESS with the same capability of active and reactive powers is installed on each node and absolute summation of all the deviation of magnitude and angle in all the buses of the system are calculated as S_{PQ} . Getting this variable requires the power flow program to run several times and ESS placement changes from node to node. The result of the comparison is shown in Fig. ?. Both of the cumulative indices have a good coloration to the actual changes in P and Q , as it was expected elimination

method has a closer match and it is a better criterion for weak node detection.

Three indices of $I_{\delta P_e}$, I_{VQ_e} , and I_{T_e} are suggested for weak node detection depending on the main function of the ESS. If the main duty is to provide/absorb active power $I_{\delta P_e}$ is the best criteria. For an STATCOM or var-compensator or to deal with the voltage drop I_{VQ_e} is the best index and cumulative index of I_{T_e} can be used if the ESS's purpose is to control and regulate both of the active and reactive powers.

5 IEEE 24-Bus System for the Comparison with the Conventional Method

IEEE 24-bus system is investigated based on the conventional iteration algorithm in [9, 10] and bus 14 is selected as the best node to install ESS. For the sake of comparison the suggested method is applied to IEEE 24-bus system and the results are shown in Fig. ?. Without any While loop or If-Then statements, simply the highest total eliminated index number is bus 14 which is the same conclusion of the conventional method.

6 IEEE 123-Bus System as a Large Network

One of the advantages of the suggested method over other methods is that as far as Newton-Raphson power flow can be applied to a network, Jacobian matrix exists, it is invert-able and the weakness of the nodes can be quantified. IEEE 123-bus distribution network is selected because of its complexity and interconnected structure. Some of the loads in this system are single phase which are substituted with their equivalent three-phase loads. Assuming the ESS have to provide/absorb both of the active and reactive power, Fig. ?? shows the network and suggested weak nodes who defined by the I_{T_e} index. The utility is connected to node 115. The suggested node is 83 which is indicated in Fig. ?? as well.

Although installing an ESS on a weak node can benefit the overall system when the ESS provides power, it should not be charged at the full rate because absorbing full power on a weak node can jeopardize the stability of the system. To show the superior of the suggested node of 83, a 150 kVA ESS is installed over nodes 83, and three other random nodes of the network which are node 114, 23, and 64. The overall angle increment of all the nodes after ESS is shown in Table ?. The overall magnitude increment, and the total of the angle and magnitude is shown as well. While installing ESS on all of these nodes have a positive effect on the angle and magnitude, installing ESS on the node 83 leads to the highest overall improvement. Angle variations are multiplied by a constant coefficient of $k = 3.2$ to add to the voltage variations.

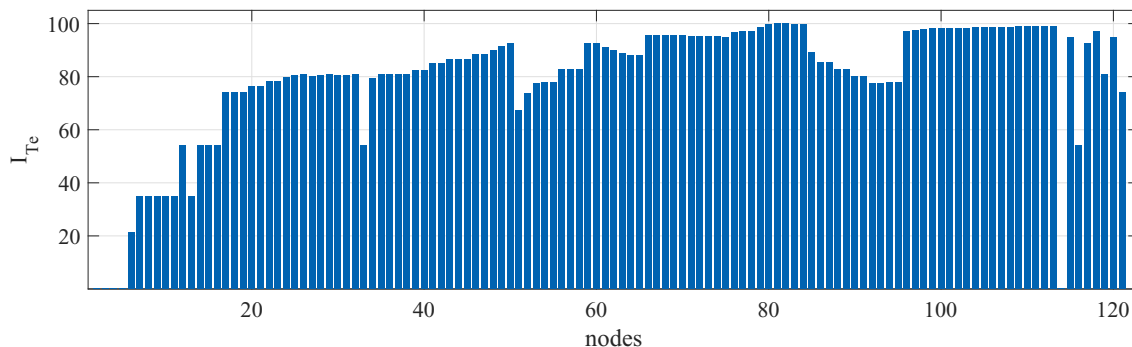


Figure 10: The total eliminated index, I_{Te} , for IEEE 123-bus system.

7 The Gravity Field of ESSs and the Case of Multiple ESSs

The total eliminated index, I_{Te} reveals the weakest node to install ESS. However, the effect of the ESS on the improving of the angle and magnitude of the network can be assessed by looking at I_{Te} after installing an ESS. It can be imagined that the ESS has a gravity field that improves the node it is connected to as well as the neighbor nodes. The amount of influence is depending on the rated capacity of the ESS.

When there are multiple ESS available to install, the second highest index cannot be used to determine the location of the second ESS because installing the first ESS, makes the weak node and all the nodes around it stronger and hence change the status of the network. Studying the gravity of an ESS helps to assess the status of the network after installing the ESS and determine the optimal location of the next possible ESS. If there is a third ESS the network needs to be reevaluated after the first two ESS and so on.

The first ESS can be considered as a new feeder and hence the nodes which the first ESS is installed can be treated as a PV node. I_{Te} needs to get recalculated. Fig. 11(a) shows the IEEE 123-bus network before installing any ESS. The difference between highest and lowest I_{Te} colors are exaggerated slightly for the sake of presentation. The utility connection is dark blue which is the strongest node and bus 83 is dark red which is determined the weakest node and the best place to install ESS. Fig. 11(b) shows the status of the system after installing an ESS in bus 83 with the rating of 6 kW and 6 kVar. Node 80 is now the best node for the second ESS and node 81 and 82 have a better status due to the gravity of the first ESS in node 83.

increasing the capacity of the first ESS from 6 to 13 kVA makes the gravity of the first ESS stronger and now more neighbor nodes are improved and hence the best location for the second ESS is farther away at node 77 as it is shown in Fig. 11(c). Increasing the capacity to 28 kVA shifts the best node to 107 and changes the overall indices of the network. Node 29 is very far from the ESS but still the I_{Te} of this node in Figs. 11(a), 11(d) are significantly different.

8 Conclusion

In this paper, a Jacobian matrix-based sensitivity method is used to quantify the weakness of nodes in a network. The most vulnerable node has the largest variation of the voltage angle and magnitude for a certain change in the active or reactive power and hence it is the ideal place to install an ESS. Unlike most of the iteration-based optimization methods, the suggested method does not require iteration loop and therefore the convergence problem is not a concern. The method is very straight forward and can be applied to any large network as far as it can be solved by Newton-Ralphson method and in this paper, the IEEE 14, 24 and 123-bus systems are studied. The method suggests indices to determine the optimal placement of an ESS which mainly provides active power rather than reactive power, a var control inverter which controls only reactive power, or any arbitrary combination of both with an ESS which regulates both active and reactive powers. A gravity approach is suggested to determine the optimal placement of multiple ESSs.

Acknowledgment

This material is based upon work supported by the National Science Foundation under Grant No. 1650470. Any opinions, findings, and conclusions or recommendations expressed in this material are those of the author(s) and do not necessarily reflect the views of the National Science Foundation.

References

- [1] G. A. Ajenikoko, "A genetic algorithm approach for optimal distribution system network reconfiguration," *International Journal of Smart Grid-ijSmartGrid*, vol. 1, no. 1, pp. 34–41, 2017.
- [2] J. Martynaitis, "Fuzzy approach for optimal placement and sizing of capacitor banks in the presence of harmonics," *IEEE Transactions on Power Delivery*, vol. 20, no. 2, pp. 1214–, Apr 2004.

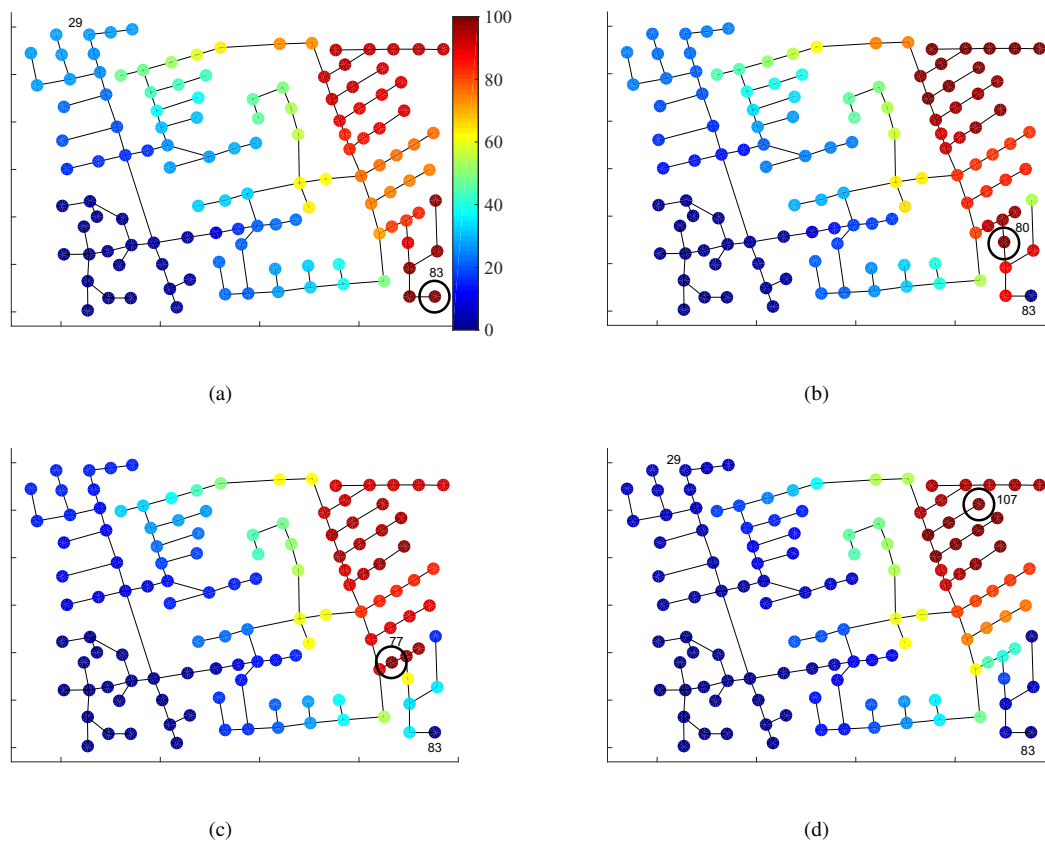


Figure 11: A gravity representation of the total eliminated index, I_{Te} , for IEEE 123-bus system.: (a) There is no ESS; (b) ESS installed at node 83 and rated for 6 kVA; (c) ESS installed at node 83 and rated for 13 kVA; and (d) ESS installed at node 83 and rated for 28 kVA.

[3] M. A. S. Masoum, M. Ladjevardi, A. Jafarian, and E. F. Fuchs, "Optimal placement, replacement and sizing of capacitor banks in distorted distribution networks by genetic algorithms," *IEEE Transactions on Power Delivery*, vol. 19, no. 4, pp. 1794–1801, Oct 2004.

[4] M. Saleh, Y. Esa, N. Onuorah, and A. A. Mohamed, "Optimal microgrids placement in electric distribution systems using complex network framework," in *2017 IEEE 6th International Conference on Renewable Energy Research and Applications (ICRERA)*, Nov 2017, pp. 1036–1040.

[5] S. Ruiz and J. Espinosa, "Multi-objective optimal sizing design of a diesel-pv-wind-battery hybrid power system in colombia," *International Journal of Smart Grid-ijSmartGrid*, vol. 2, no. 1, pp. 49–57, 2018.

[6] M. R. Tur and R. Bayindir, "Project surveys for determining and defining key performance indicators in the development of smart grids in energy systems," *International Journal of Smart Grid-ijSmartGrid*, vol. 3, no. 2, pp. 103–107, 2019.

[7] A. Keane and M. O'Malley, "Optimal allocation of embedded generation on distribution networks," *IEEE Transactions on Power Systems*, vol. 20, no. 3, pp. 1640–1646, Aug 2005.

[8] G. Carpinelli, G. Celli, S. Mocci, F. Mottola, F. Pilo, and D. Proto, "Optimal integration of distributed energy storage devices in smart grids," *IEEE Transactions on Smart Grid*, vol. 4, no. 2, pp. 985–995, Jun 2013.

[9] M. Ghofrani, A. Arabali, M. Etezadi-Amoli, and M. S. Fadali, "A framework for optimal placement of energy storage units within a power system with high wind penetration," *IEEE Transactions on Sustainable Energy*, vol. 4, no. 2, pp. 434–442, Apr 2013.

[10] —, "Energy storage application for performance enhancement of wind integration," *IEEE Transactions on Power Systems*, vol. 28, no. 4, pp. 4803–4811, Nov 2013.

[11] J. H. Teng, C. Y. Chen, and I. C. Martinez, "Utilising energy storage systems to mitigate power system vulnerability," *IET Generation, Transmission Distribution*, vol. 7, no. 7, pp. 790–798, Jul 2013.

[12] S. Pazouki, A. Mohsenzadeh, M. R. Haghifam, and S. Ardalan, "Simultaneous allocation of charging stations and capacitors in distribution networks improving voltage

- and power loss,” *Canadian Journal of Electrical and Computer Engineering*, vol. 38, no. 2, pp. 100–105, Spring 2015.
- [13] T. Sakagami, Y. Shimizu, and H. Kitano, “Exchangeable batteries for micro evs and renewable energy,” in *2017 IEEE 6th International Conference on Renewable Energy Research and Applications (ICRERA)*, Nov 2017, pp. 701–705.
- [14] J. Pegueroles-Queralt, F. D. Bianchi, and O. Gomis-Bellmunt, “A power smoothing system based on supercapacitors for renewable distributed generation,” *IEEE Transactions on Industrial Electronics*, vol. 62, no. 1, pp. 343–350, Jan 2015.
- [15] S. Bayhan, Y. Liu, and S. Demirbas, “A novel energy management algorithm for islanded ac microgrid with limited power sources,” in *2017 IEEE 6th International Conference on Renewable Energy Research and Applications (ICRERA)*, Nov 2017, pp. 64–69.
- [16] B. Cheng and W. Powell, “Co-optimizing battery storage for the frequency regulation and energy arbitrage using multi-scale dynamic programming,” *IEEE Transactions on Smart Grid*, vol. PP, no. 99, pp. 1–1, 2017.
- [17] Y. Niu and S. Santoso, “Sizing and coordinating fast- and slow-response energy storage systems to mitigate hourly wind power variations,” *IEEE Transactions on Smart Grid*, vol. PP, no. 99, pp. 1–1, 2017.
- [18] D. Fooladivanda, C. Rosenberg, and S. Garg, “Energy storage and regulation: An analysis,” *IEEE Transactions on Smart Grid*, vol. 7, no. 4, pp. 1813–1823, Jul 2016.
- [19] Y. Shimizu, T. Sakagami, and H. Kitano, “Prediction of weather dependent energy consumption of residential housings,” in *2017 IEEE 6th International Conference on Renewable Energy Research and Applications (ICRERA)*, Nov 2017, pp. 967–970.
- [20] C. K. Chau, G. Zhang, and M. Chen, “Cost minimizing on-line algorithms for energy storage management with worst-case guarantee,” *IEEE Transactions on Smart Grid*, vol. 7, no. 6, pp. 2691–2702, Nov 2016.
- [21] M. Zeraati, M. E. H. Golshan, and J. Guerrero, “Distributed control of battery energy storage systems for voltage regulation in distribution networks with high pv penetration,” *IEEE Transactions on Smart Grid*, vol. PP, no. 99, pp. 1–1, 2016.
- [22] P. M. van de Ven, N. Hegde, L. Massouli, and T. Salonidis, “Optimal control of end-user energy storage,” *IEEE Transactions on Smart Grid*, vol. 4, no. 2, pp. 789–797, Jun 2013.
- [23] K. Rahbar, J. Xu, and R. Zhang, “Real-time energy storage management for renewable integration in microgrid: An off-line optimization approach,” *IEEE Transactions on Smart Grid*, vol. 6, no. 1, pp. 124–134, Jan 2015.
- [24] S. Wen, H. Lan, Q. Fu, D. C. Yu, and L. Zhang, “Economic allocation for energy storage system considering wind power distribution,” *IEEE Transactions on Power Systems*, vol. 30, no. 2, pp. 644–652, Mar 2015.
- [25] M. H. Athari, Z. Wang, and S. H. Eylas, “Time-series analysis of photovoltaic distributed generation impacts on a local distributed network,” in *2017 IEEE Manchester PowerTech*, June 2017, pp. 1–6.
- [26] F. Mohammadi, H. Gholami, G. B. Gharehpetian, and S. H. Hosseinian, “Allocation of centralized energy storage system and its effect on daily grid energy generation cost,” *IEEE Transactions on Power Systems*, vol. 32, no. 3, pp. 2406–2416, May 2017.
- [27] Q. Sun, B. Huang, D. Li, D. Ma, and Y. Zhang, “Optimal placement of energy storage devices in microgrids via structure preserving energy function,” *IEEE Transactions on Industrial Informatics*, vol. 12, no. 3, pp. 1166–1179, Jun 2016.
- [28] C. Thrampoulidis, S. Bose, and B. Hassibi, “Optimal placement of distributed energy storage in power networks,” *IEEE Transactions on Automatic Control*, vol. 61, no. 2, pp. 416–429, Feb 2016.
- [29] S. G. Ghiocel and J. H. Chow, “A power flow method using a new bus type for computing steady-state voltage stability margins,” *IEEE Transactions on Power Systems*, vol. 29, no. 2, pp. 958–965, Mar 2014.